Theoretical analysis and simulation of growth rate and start current in Smith–Purcell free-electron lasers

D. Li [1*], M. Hangyo [2], Z. Yang [3], Y. Tsunawaki [4], Y. Wei [3], Y. Wang [3], S. Miyamoto [5], M. R. Asakawa [4], and K. Imasaki [1]

[1] Institute for Laser Technology, Suita, Osaka 565-0871, Japan

[2] Institute of Laser Engineering, Osaka University, Suita, Osaka 565-0871, Japan

[3] School of Physical Electronics, University of Electronic Science and Technology of China, Chengdu 610054, China

[4] Department of Pure and Applied Physics, Faculty of Engineering Science, Kansai University, Osaka 564-8680, Japan

[5] Laboratory of Advanced Science and Technology for Industry, University of Hyogo, Ako, Hyogo 678-1205, Japan

[*1] Email: Dazhi_li@hotmail.com

(Received March 08, 2013)

Abstract: We present an analytical theory for small-signal operation of a Smith–Purcell free-electron laser with a finitely thick electron beam travelling close to the surface of a grating. The dispersion equation is derived from a self-consistent set of small-signal equations describing the dynamics of beam-wave interaction. Through the analysis of the power flow above the grating, the mechanism of beam-wave interaction in the device is explored. By solving the dispersion equation carefully, we reveal that the growth rate of the field amplitude holds a finite value at the Bragg point, which is different from previous theoretical predictions. After deriving an approximate equation to calculate the growth rate, the oscillation start current of the device is worked out by considering the power flow above the grating. The predictions of our theory are compared with those of particle-in-cell simulations, and the agreement is reasonable.

Keywords: Smith–Purcell free-electron laser, Growth rate, Start current, Particle-in-cell simulation

doi: 10.11906/TST.189-205.2013.09.13

1. Introduction

When an electron beam passes over a diffraction grating, it emits Smith–Purcell radiation, which was first observed by Smith and Purcell in 1953 [1]. Due to the properties of Smith–Purcell radiation, since 1970s, it has been considered as a promising mechanism by which a compact radiation source can generate millimeter and sub-millimeter waves [2-5]. It is believed that a compact, tunable, and coherent radiation source in the THz domain could be developed using the principles of Smith–Purcell free-electron lasers [6-14].

The principle of the beam-wave interaction above an open grating was established in Refs. [7-9], where the authors assumed a uniform electron beam filling the entire space above a lamellar grating and derived the dispersion relation. The authors pointed out that the device

operates as a backward-wave oscillator (BWO) when the interaction with an electron beam occurs on the downward slope of the dispersion relation and as a travelling-wave tube (TWT) when the interaction occurs on the upward slope. From their theory, they predicted that the spatial growth rate would be proportional to $I^{1/3}v_g^{-1/3}$, where I is the beam current and $v_g = d\omega/dk$ is the group velocity of the surface wave, and that the growth rate diverges at the Bragg point, where the group velocity vanishes. Because the external feedback is not necessary for the operation of a BWO, the research on Smith–Purcell free-electron lasers has been focused on a BWO-type device. When the beam current exceeds a threshold called start current, the beam-wave interaction leads to beam bunching. If the bunching is strong enough, coherent radiation at the harmonic frequencies of the bunching frequency could be emitted around the corresponding Smith–Purcell angle [7-9]. In evaluating the start current of the BWO-type device, all the authors followed the methods that have been used for analyzing BWOs in Refs. [15-17]. Almost the same boundary conditions were used in Refs. [8-14] to establish the equations determining the start current. One condition, namely, the field vanishes at the downstream end of the grating, is based on the assumption that there is no input field.

However, in a recent experiment performed to measure start current and growth rate [18], the authors found that the best fit to their experimental data and simulations of growth rate is $I^{1/2}$ and, for higher currents, $I^{1/3}$. From our previously published paper [19], we know that it is possible for the surface wave to interact with the electron beam even at the Bragg point, so the prediction given in Refs. [8, 9] that the growth rate diverges at the Bragg point cannot be true. Also, the behavior that occurs at the ends of a grating, which will be addressed later, and the effect of this behavior in determining start current implies that the condition of a vanishing electromagnetic field at the downstream end is less reasonable. Therefore, considering the current interest in developing Smith–Purcell free-electron lasers, it is necessary to reexamine the theoretical analysis.

We derived a dispersion equation based on a scheme with an electron beam passing over a lamellar grating. An approximate equation for calculating the growth rate was worked out from the dispersion equation. By our theory, the growth rate is not divergent at the Bragg point, which differs from that predicted in Refs. [8, 9]. We also developed a simple approach to evaluate the start current by analyzing the power flow above the grating. Finally, particle-in-cell simulations were performed to examine the predictions of our theory. This theory was simply described in our previous paper [20], where the case of magnetized electron beam was analyzed. In this paper, we introduce this theory in details through studying the case of which the electron beam was not magnetized. Though an electron beam of finite thickness was previously analyzed in Ref. [21], the author did not take into account the growth rate at the Bragg point or start current.

2. Dispersion

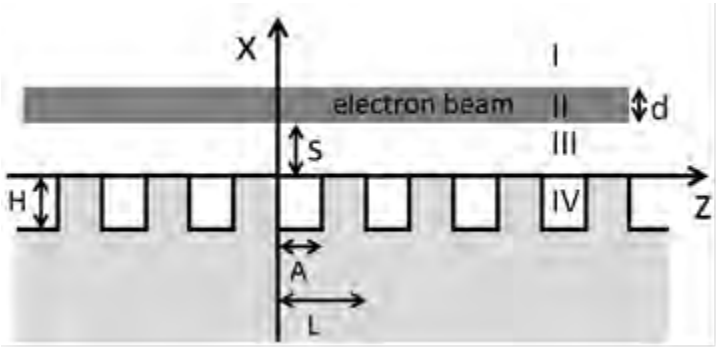

Fig. 1 Schematic of Smith–Purcell free-electron laser by an electron beam with finite thickness moving parallel to the surface of a grating with rectangular grooves.

In the Cartesian coordinate system shown in Fig. 1, the electrons initially move in the z direction with velocity v_0 in the vacuum above the grating along the trajectories $s \le x \le s + d$, and are coupled with the TM mode of an electromagnetic wave. The grating is ruled parallel to the y direction, and it has a period length L, groove width A, and groove depth H. Both the geometry of the configuration and all field quantities are independent of the y direction, making this problem two dimensional. The grating is assumed to be a perfect conductor, which means that the losses from the surface current can be ignored. Following the methods using in Ref. [22] and considering the fields with time dependence $e^{j\omega t}$, we get the self-consistent set of Maxwell and fluid equations:

$$\partial_x E_z - \partial_z E_x = j\omega B_y \tag{1a}$$

$$\partial_z B_y = -j\frac{\omega}{c^2}E_x + e\mu_0 n_0 v_x \tag{1b}$$

$$\partial_x B_y = j\frac{\omega}{c^2}E_z - e\mu_0(n_0 v_z + n v_0) \tag{1c}$$

$$\partial_x E_x + \partial_z E_z = -\frac{e}{\varepsilon_0}n \tag{1d}$$

$$j\omega\delta v_x + v_0\partial_z\delta v_x = \frac{-e}{\gamma m_0}(E_x - v_0 B_y) \tag{1e}$$

$$j\omega\delta v_z + v_0\partial_z\delta v_z = \frac{-e}{\gamma m_0}(E_z - \frac{v_0^2}{c^2}E_z) \tag{1f}$$

$$v_0\partial_z\delta n + (\frac{\partial}{\partial x}\delta v_x + \partial_z\delta v_z)N_0 = -j\omega\delta n \tag{1g}$$

where $-e$ is the electronic charge, v_0 is the drift velocity of the electron beam, c is the velocity of light in a vacuum, and v_x and v_z denote the x and z components of the small-signal velocity, respectively. In addition, n_0 and n express the average number density and small-signal number density of electrons, respectively. According to Floquet's theorem, the component of magnetic-flux density above the grating in y direction B_y can be expanded in the form

$$B_y = \sum_{p=-\infty}^{\infty} B_p(x) e^{-jk_p z}, \tag{2}$$

where $k_p = k + 2\pi p/L$, and p is an integer. Substitute Eq. (2) into Eq. (1), and we get the relations between electric fields and magnetic-flux density B_y,

$$E_x = \frac{jc^2\varepsilon_x}{\omega}\frac{\partial B_y}{\partial z}, \quad E_z = \frac{c^2}{j\omega\varepsilon_z}\frac{\partial B_y}{\partial x}, \tag{3}$$

where

$$\varepsilon_x = \frac{\omega - v_0 k_p - \dfrac{v_0\omega_p^2}{c^2 k_p}}{\omega - v_0 k_p - \dfrac{\omega_p^2}{\omega}}, \quad \varepsilon_z = 1 - \frac{\omega_p^2}{\omega(\omega - v_0 k_p)}, \quad \omega_p^2 = \frac{n_0 e^2}{\gamma m_0 \varepsilon_0}, \gamma = \frac{1}{\sqrt{1-\beta^2}}, \quad \beta = \frac{v_0}{c},$$

and the wave equation is obtained below:

$$\frac{\partial^2}{\partial x^2} B_p(x) - (k_p^2 - \frac{\omega^2}{c^2} + \frac{\omega_p^2}{c^2}) B_p(x) = 0. \tag{4}$$

In Region (I), the solution of the wave equation can be written as

$$B_p^{(I)}(x) = B_{I,p} e^{-\alpha_p x},$$

where $B_{I,p}$ is a constant and $\alpha_p^2 = k_p^2 - \omega^2/c^2$. In Region (II), where the electron beam exists, we get

$$B_p^{(II)}(x) = B_{II,p}^{+} e^{\alpha_{II} x} + B_{II,p}^{-} e^{-\alpha_{II} x},$$

where $\alpha_{II}^2 = k_p^2 - \omega^2/c^2 + \omega_p^2/c^2$. In Region (III), the solution can be written in the form

$$B_p^{(III)}(x) = B_{III,p}^{+} e^{\alpha_p x} + B_{III,p}^{-} e^{-\alpha_p x}.$$

Using the relation expressed by Eq. (3), we can obtain other fields in each region.

Region I:

$$B_y^{(I)} = \sum_{p=-\infty}^{\infty} B_{I,p} e^{-\alpha_p x} e^{-jk_p z} \tag{5a}$$

$$E_x^{(I)} = \sum_{p=-\infty}^{\infty} B_{I,p} \frac{c^2 k_p}{\omega} e^{-\alpha_p x} e^{-jk_p z} \tag{5b}$$

$$E_z^{(I)} = \sum_{p=-\infty}^{\infty} B_{I,p} \frac{jc^2 \alpha_p}{\omega} e^{-\alpha_p x} e^{-jk_p z} \tag{5c}$$

Region II:

$$B_y^{(II)} = \sum_{p=-\infty}^{\infty} (B_{II,p}^{+} e^{\alpha_{II} x} + B_{II,p}^{-} e^{-\alpha_{II} x}) e^{-jk_p z} \tag{6a}$$

$$E_x^{(II)} = \sum_{p=-\infty}^{\infty} \frac{c^2 k_p \varepsilon_x}{\omega} (B_{II,p}^{+} e^{\alpha_{II} x} + B_{II,p}^{-} e^{-\alpha_{II} x}) e^{-jk_p z} \tag{6b}$$

$$E_z^{(II)} = \sum_{p=-\infty}^{\infty} \frac{-jc^2 \alpha_{II}}{\omega \varepsilon_z} (B_{II,p}^{+} e^{\alpha_{II} x} - B_{II,p}^{-} e^{-\alpha_{II} x}) e^{-jk_p z} \tag{6c}$$

Region III:

$$B_y^{(III)} = \sum_{p=-\infty}^{\infty} (B_{III,p}^{+} e^{\alpha_p x} + B_{III,p}^{-} e^{-\alpha_p x}) e^{-jk_p z} \tag{7a}$$

$$E_x^{(III)} = \sum_{p=-\infty}^{\infty} \frac{c^2 k_p}{\omega} (B_{III,p}^{+} e^{\alpha_p x} + B_{III,p}^{-} e^{-\alpha_p x}) e^{-jk_p z} \tag{7b}$$

$$E_z^{(III)} = \sum_{p=-\infty}^{\infty} \frac{-jc^2\alpha_p}{\omega\varepsilon_z}(B_{III,p}^{+}e^{\alpha_p x} - B_{III,p}^{-}e^{-\alpha_p x})e^{-jk_p z} \tag{7c}$$

Next, we consider the boundary conditions at the surface between the vacuum and the electron beam. Taking into account the surface current, the boundary conditions at $x = s + d$ are given as [22]

$$E_z^{(I)} = E_z^{(II)},$$

$$B_y^{(I)} - B_y^{(II)} = \frac{v_0}{c^2}(E_x^{(I)} - E_x^{(II)}).$$

In addition, at $x = s$, they are

$$E_z^{(II)} = E_z^{(III)},$$

$$B_y^{(II)} - B_y^{(III)} = \frac{v_0}{c^2}(E_x^{(II)} - E_x^{(III)}).$$

Substituting Eqs. (5)–(7) into the above conditions, we achieve

$$B_{III,p}^{+} = g_p B_{III,p}^{-}, \tag{8}$$

where

$$g_p = \frac{(e^{2\alpha_{II}d} - 1)(\alpha_p^2\varepsilon_z^2(k_p v_0\varepsilon_x - \omega)^2 - \alpha_{II}^2(v_0 k_p - \omega)^2)}{e^{2\alpha_p s}((\alpha_p\varepsilon_z(k_p v_0\varepsilon_x - \omega) + \alpha_{II}(v_0 k_p - \omega))^2 e^{2\alpha_{II}d} - (\alpha_p\varepsilon_z(k_p v_0\varepsilon_x - \omega) - \alpha_{II}(v_0 k_p - \omega))^2)}.$$

In the grooves of the grating, we expand the magnetic-flux density using a Fourier series:

$$B_y^g = \sum_{n=0}^{\infty} B_{g,n}\cos(\frac{n\pi z}{A})(\cos(\alpha_{g,n}x) - \tan(\alpha_{g,n}H)\sin(\alpha_{g,n}x)),$$

where $\alpha_{g,n}^2 = (\omega/c)^2 - (n\pi/A)^2$. It has been shown that the dispersion relation can be accurately described (within a few percent) even if just the fundamental mode is used [8]. Therefore, for simplicity and without loss of generality, we only take the fundamental mode ($n = 0$) in the groove, which is the most easily excited mode. Then, we get

$$B_y^g = B_{g,0}(\cos(\alpha_{g,0}x) - \tan(\alpha_{g,0}H)\sin(\alpha_{g,0}x)), \tag{9}$$

and the corresponding electric field is written as

$$E_z^g = \frac{jc^2}{\omega} B_{g,0}(\sin(\alpha_{g,0}x) + \tan(\alpha_{g,0}H)\cos(\alpha_{g,0}x)). \tag{10}$$

Across the interface between the grating and the electron beam, the tangential component of the electric field should be continuous. Since the tangential field vanishes on the surface of the conductor, we get

$$\sum_{p=-\infty}^{\infty} \frac{-jc^2\alpha_p}{\omega\varepsilon_z}(B_{III,p}^{+}e^{\alpha_p x} - B_{III,p}^{-}e^{-\alpha_p x})e^{-jk_p z} = \begin{cases} \frac{jc^2}{\omega} B_{g,0}(\sin(\alpha_{g,0}x) + \tan(\alpha_{g,0}H)\cos(\alpha_{g,0}x)) & for 0 < z < A \\ 0 & for A < z < L \end{cases}. \tag{11}$$

If we multiply Eq. (11) by $e^{jk_q z}$ and integrate over $0 < z < L$, we can get

$$B_{III,q}^{-} = \frac{-B_{g,0}\alpha_{g,0}\tan(\alpha_{g,0}H)S_{1,q}}{\alpha_q L(g_q - 1)}, \tag{12}$$

where

$$S_{1,q} = \int_0^A e^{jk_q z} dz.$$

Likewise, the tangential component of the magnetic-flux density must be continuous across the interface, so we have

$$\sum_{p=-\infty}^{\infty}(B_{III,p}^{+}e^{\alpha_p x} + B_{III,p}^{-}e^{-\alpha_p x})e^{-jk_p z} = B_{g,0}(\cos(\alpha_{g,0}x) - \tan(\alpha_{g,0}H)\sin(\alpha_{g,0}x)). \tag{13}$$

If we integrate Eq. (13) over $0 < z < A$, we get

$$B_{g,0} = \sum_{p=-\infty}^{\infty} \frac{(g_p + 1)B_{III,p}^{-}S_{2,p}}{A}, \tag{14}$$

where

$$S_{2,p} = \int_0^A e^{jk_p z} dz .$$

Replacing q in Eq. (12) with p and substituting it into Eq. (14), we obtain the dispersion equation:

$$\sum_{p=-\infty}^{\infty} \Re_p \frac{\alpha_{g,0} \tan(\alpha_{g,0} d) S_{1,p} S_{2,p}}{LA\alpha_p} = 1. \tag{15}$$

Here,

$$\Re_p = \frac{1+g_p}{1-g_p}. \tag{16}$$

For the case of absence of electron beam, ω_p vanishes and the dispersion equation is simplified as

$$\sum_{p=-\infty}^{\infty} \frac{\alpha_{g,0} \tan(\alpha_{g,0} d) S_{1,p} S_{2,p}}{LA\alpha_p} = 1. \tag{17}$$

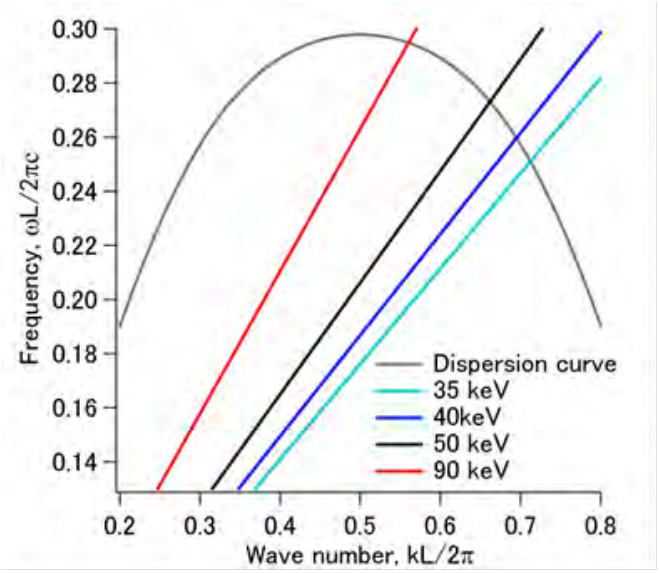

Fig. 2 Dispersion relation of the surface wave for the grating. The operating point is the intersection of the frequency curve with the beam line.

The grating parameters used in this paper are set to be L = 173 μm, A = 62 μm, H = 100 μm, and the period number of 73, which are the same as the experiments reported in Ref. [6]. Using these parameters, the dispersion relation is obtained by numerically solving Eq. (17), and the result is shown in Fig. 2, which shows that the operating point (ω_0, k_0) of the laser is where beam line βk intersects the dispersion curve. It also shows that for electrons with energy of 90 keV, the intersection occurs on the downward slope. We carried $-4 \le p \le 4$ in the expansion of Eq. (17), which showed good convergence.

We know that a surface mode consists of the superposition of an infinite number ($p = -\infty..\infty$) of spatial harmonics, and that those with positive k_p carry energy flow forward, while those with negative k_p carry energy flow backward. From the dispersion equation, we can calculate relative amplitudes of the first few spatial harmonics and, consequently, can calculate the average power carried by each harmonic

$$S_p = \int_0^\infty dx \frac{1}{2} E_{x,p} H_{y,p}^* = \frac{1}{4} \frac{c^2 k_p B_{l,p}^2}{\omega \mu_0 \alpha_p}. \tag{18}$$

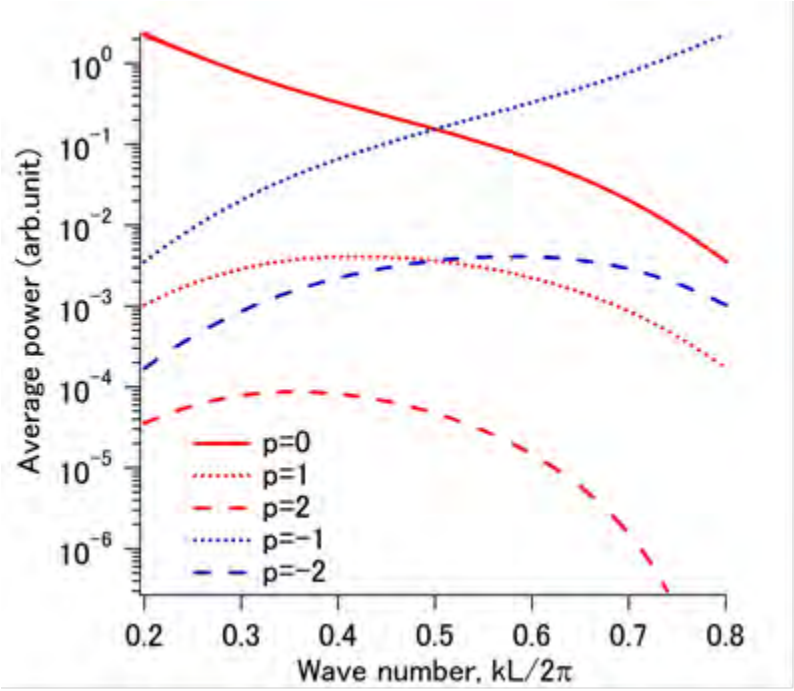

Fig. 3 Average power of the first few space harmonics. Note that S_{-1} and S_{-2} are actually with negative value, meaning that energy flows backward.

The results are as shown in Fig. 3, where we plot the absolute value of normalized S_p for

convenient comparison (amplitude of the field is normalized to B_g), and note that S_{-1} and S_{-2} are actually negative, meaning that energy flows backward. From Fig. 3, we know that the zeroth and –1st order harmonics hold most of the energy of the surface wave. For the downward slope in Fig. 2, the total power flow is backward which leads to negative group velocity, while for the upward slope the total power flow is forward which leads to positive group velocity. At the central point $kL/2\pi$ = 0.5, i.e., Bragg point, the group velocity is zero, which means that the forward power flow equals the backward flow.

3. Spatial growth rate

To compute the amplitude growth rate, we should directly solve Eq. (15). Usually, Eq. (15) can be simplified as discussed below [8, 9, 21]. We know that only the zeroth space harmonic can synchronize with the electron beam; thus, it is reasonable to only consider $\Re_{p=0}$ near the operating point (ω_0, k_0). Also, if the beam density is small enough, $\Re_{p=0}$ can be expanded in powers of small magnitude $\frac{\omega_b^2}{\gamma^3(\omega - kv_0)^2}$, where $\omega_b^2 = \gamma\omega_p^2$. Then, Eq. (15) can be simplified to be

$$\xi - 1 + \Theta\Omega = 0 \tag{19}$$

where

$$\xi = \sum_{p=-\infty}^{\infty} \frac{\alpha_{g,0}\tan(\alpha_{g,0}d)S_{1,p}S_{2,p}}{LA\alpha_p} \quad , \quad \Omega = \frac{\alpha_{g,0}\tan(\alpha_{g,0}d)S_{1,0}S_{2,0}}{LA\alpha_0} \quad , \quad \Theta = \sum_{n=1}^{\infty} \frac{\mathrm{X}^n \Re_{p=0}^{(n)}(0)}{n!} \quad ,$$

$$\mathrm{X} = \frac{\omega_b^2}{\gamma^3 v_0^2 \delta k^2}, \delta k = k - k_0,$$

and $\Re_{p=0}^{(n)}(0)$ is the nth derivative of $\Re_{p=0}$ at 0. Note that the beam density should satisfy the conditions $\omega_b / \omega\sqrt{\gamma} << 1$ and $\omega_b^2 / (\gamma^3 v_0^2 \delta k^2) << 1$ in the simplifying process.

Next, we can expand ξ at the operating point (ω_0, k_0). If we take the first order of expanded powers, Eq. (19) can be written as

$$\xi'(\omega_0, k_0)\delta k + (e^{-2\alpha_0 d} - 1)e^{-2\alpha_0 s}\Omega \frac{\omega_b^2}{\gamma^3 \beta^2 c^2 \delta k^2} = 0, \tag{20}$$

where $\xi'(\omega_0, k_0)$ is the derivative $\partial\xi/\partial k$ at (ω_0, k_0).

From the above equations, obtaining the spatial growth rate is straightforward:

$$\mu = \mathrm{Im}(\delta k) = \frac{\sqrt{3}}{2}\left| -\frac{(e^{-2\alpha_0 d} - 1)e^{-2\alpha_0 s}\Omega\omega_b^2}{\gamma^3\beta^2c^2\xi'(\omega_0, k_0)} \right|^{\frac{1}{3}}. \tag{21}$$

If we take $s = 0$ and $d -> \infty$, i.e., an infinitely thick electron beam, Eq. (21) would be analogous to the growth rate obtained in Refs. [8, 9].

Eq. (21) shows that the growth rate diverges at the Bragg point where $\xi'(\omega_0, k_0)$ vanishes. However, this is not due to the actual physics that occurred there but is instead due to the rough mathematical calculation. If we take into account more terms of expansion, the growth rate would have a finite value at any point on the dispersion curve. We try to attain better precision with fewer terms of expanded powers. In this paper, we expand ξ and Θ up to the second order; thus, Eq. (19) should be rewritten as

$$\sum_{n=1}^{2}\frac{\delta k^n \xi^{(n)}(\omega_0, k_0)}{n!} + \Omega\cdot\sum_{n=1}^{2}\frac{\mathrm{X}^n \Re_{p=0}^{(n)}(0)}{n!} = 0. \tag{22}$$

This equation can be numerically solved to obtain δk, and $\mathrm{Im}(\delta k)$ would be the spatial growth rate . Eq. (22) is a sixth-order equation, and hence, strictly speaking, the spatial growth rate is not proportional to $I^{1/3}$. Eq.(22) has six solutions. One of them that has the maximum imaginary part indicates the mainly growing mode, and the other solutions can be neglected.

We have made calculations for the grating parameters mentioned above. We assume that the electron beam fills a region of width d = 24 μm, equal to the diameter of the beam used in Ref.[6]. Beam height above the grating and the beam energy are assumed to be s = 30 μm and E_b = 90 keV, respectively. In these calculations, the beam current is fixed to $I = 1$ mA, and we have the relation

$$\omega_b^2 = \frac{Ie_0}{m_0\varepsilon_0\beta c d^2},$$

where m_0 is the electron mass, and d is the thickness and width of the electron beam. The results are shown in Fig. 4, where the spatial growth rate is a function of beam energy. As shown in Fig. 4, according to the previous theory, the growth rate diverges when the electron beam

energy reaches 124 *keV*, i.e., the Bragg point; in contrast, our theory gives a finite value.

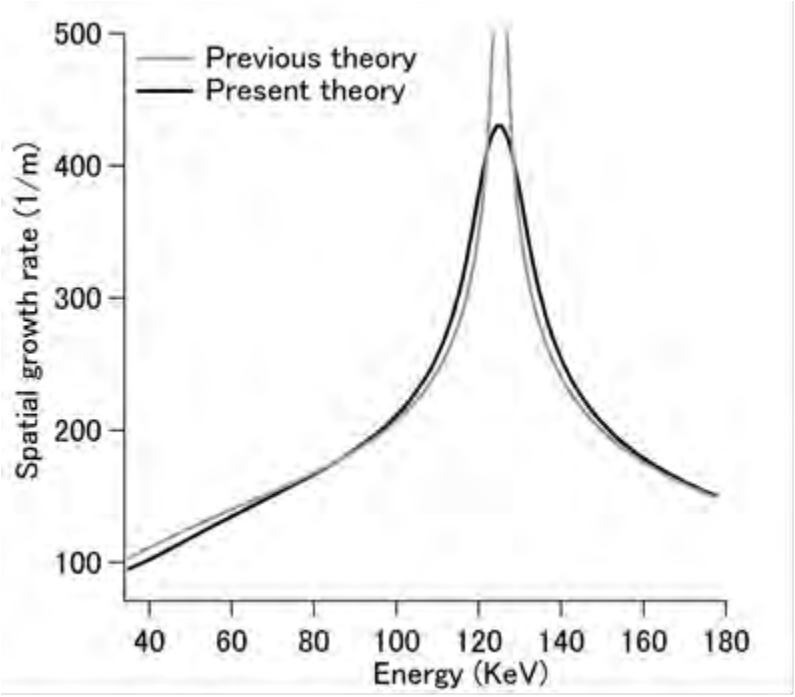

Fig. 4 Spatial growth rate (per unit distance) versus beam energy: present theory (black curve), and previous theory (gray curve).

4. Start current and temporal growth rate

As mentioned above, for $p \geq 0$, the energy-carrying space harmonics move in the z direction, while when $p < 0$, they move in the –z direction. When the device operates on the downward slope of dispersion curve, the –z-directed energy is greater than the z-directed energy, and they are equal at the Bragg point. So, in our theory, the mechanism of beam-wave interaction should occur like this: the zeroth order space harmonic interacts with the electron beam moving in the z direction and the whole harmonics are amplified during the interaction; at the downstream end, the $p \geq 0$ harmonics go out the grating (where they are partially reflected and partially diffracted; however, we ignore these reflections in the present theory), while the $p < 0$ harmonics are retained. Note that they are retained but not *reflected,* because $p < 0$ harmonics intrinsically move in the –z direction; energy carried by $p < 0$ harmonics are reapportioned among the whole harmonics to satisfy the boundary condition on the surface of a grating; in addition, at the upstream end, $p \geq 0$ harmonics are retained, and they start the second round trip. Because the zeroth and –1st order harmonics hold most of the energy of the surface wave and because they are faster than the other space harmonics, it is reasonable to consider only these two

harmonics in the following analysis.

The power flow of a space harmonic wave is expressed as Eq. (18), and we define the total power flow of the whole space harmonics as $S_{total} = \sum_{p=-\infty}^{\infty} |S_p|$. The ratio of a given harmonic to the total power flow is written as $\rho_p = |S_p| / S_{total}$. Thus, the condition for device to start oscillating should be $S_{total}(z=0) \cdot e^{2\mu\ell} \cdot \rho_{-1} \cdot \rho_0 = S_{total}(z=0)$, which can be simplified as $e^{2\mu\ell} \cdot \rho_{-1} \cdot \rho_0 = 1$, where ℓ is the total length of a grating. From the no-beam dispersion equation, we can calculate ρ_p at operating point (ω_0, k_0); thus the required spatial growth rate for starting oscillation can be acquired. Then, we can work out the start current with the help of Eq. (22). In Ref. 8, 9 and 11, the authors claimed that the interaction mechanism on the upward slope of the dispersion relation is different from that on the downward slope, and they called them travelling wave manner and backward wave manner, respectively. But, in our theory, the interaction mechanism is same. The device can oscillate without external reflections on the downward slope, the Bragg point and the upward slope of the dispersion relation when the beam current beyond the start current.

In a round trip, the fields are amplified only when the zero[th] order harmonic moves forward with the electron beam; therefore, the gain of the field can be written as a function of time $e^{(\mu\ell + \frac{1}{2}\ln(\rho_0\rho_{-1}))\frac{t}{t_e}}$, where t_e is the effective time. In addition, we know that the energy is brought back to the upstream end mainly by the –1[st] order harmonic, so the relation between effective time t_e and real time t can be easily worked out as $t_e = \frac{|v_{-1}| + v_0}{|v_{-1}| \cdot v_0}\ell$. Here, v_p is phase velocity for a p[th] order harmonic and also the energy velocity of the harmonic. Finally, we get the temporal growth rate as

$$\sigma = (\mu + \frac{1}{2\ell}\ln(\rho_{-1}\rho_0))\frac{v_0|v_{-1}|}{|v_{-1}| + v_0}. \quad (23)$$

5. Comparison with simulations

The particle-in-cell simulations for a Smith-Purcell free-electron laser have been reported in many papers [23-27]. In this paper, the simulations are carried out with using CHIPIC code [28], which is a finite-difference, time-domain code designed to simulate plasma physics processes. The grating system is assumed to be perfect conductor, and it has uniform rectangular grooves along the y direction, with parameters mentioned above. A sheet electron beam with the thickness

of 24 μm propagates along the z direction, and its bottom is over the grating surface by height of 30 μm in order to avoid the electrons hitting on the grating surface. It is a perfect beam produced from a small cathode located at the left boundary of the simulation area with energy of 90 *keV*. The beam wave interaction and radiation propagation occur in the vacuum box, which is enclosed with absorber regions. Since it is a two-dimensional simulation, it is assumed that all fields and currents are independent of the y direction. The method of extracting the temporal growth rate from the simulations has been introduced and used elsewhere [23-27], and the start current is determined by gradually decreasing or increasing the electron beam current to find the starting point of oscillation. As mentioned in Ref. 18, in the two-dimensional simulations, the relevant current is actually a linear current density whose dimension is A/m. If the beam width is taken as 24 μm, the true linear current density should be 4.17 x 10^4 times larger.

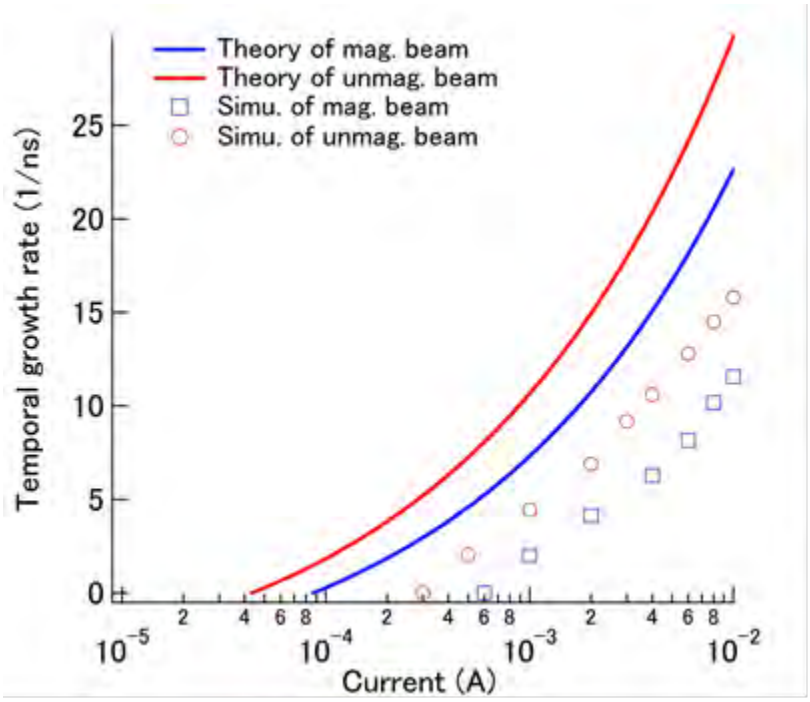

Fig. 5 Temporal growth rate and start current for 90 *keV* electron beam obtained by the present theory and simulations.

The data from simulations are given in Fig. 5, where we also plot the calculation results of Eq. 23 for comparison. Considering the simplified solution of the dispersion equation and the error in abstracting the data from simulations, we think the agreement is acceptable. To examine the conditions that the beam density should be satisfied, we made calculations corresponding to Fig. 5 and show them in Fig. 6. It is shown that $\omega_b / \omega\sqrt{\gamma} << 1$ can be well satisfied when the beam current below 10 *mA*, while $\omega_b^2 / (\gamma^3 v_0^2 \delta k^2) << 1$ can be only roughly satisfied when the beam current below 1 *mA* , and we think that this is one of the reasons leading to the differences in Fig. 5.

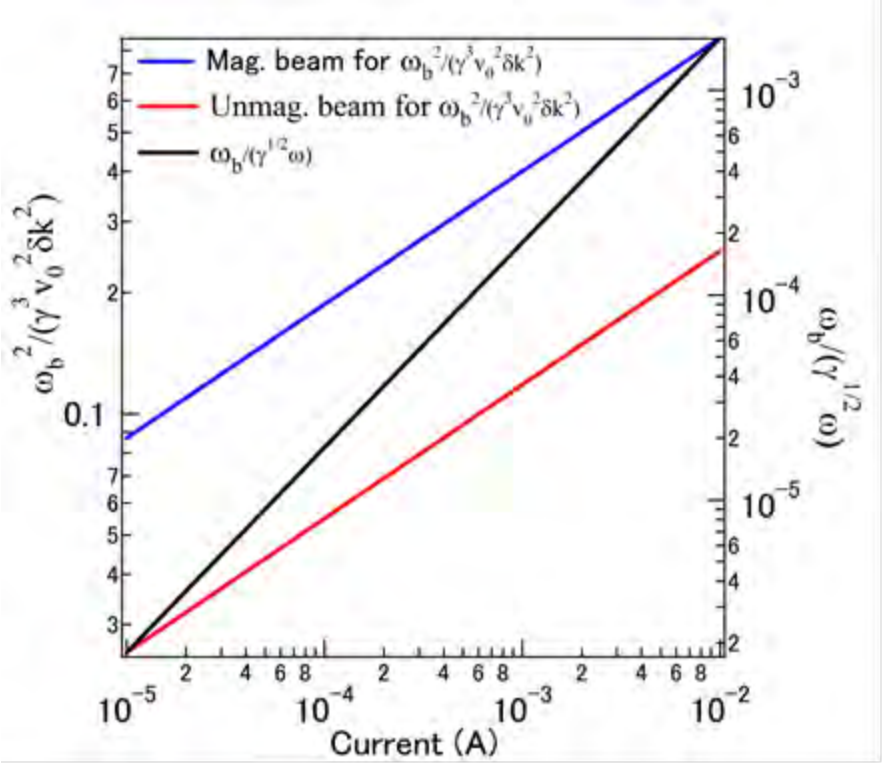

Fig. 6 Criteria of beam density for examining the reasonability of calculations shown in Fig. 5.

6. Conclusion

In conclusion, we find that forward-moving and backward-moving electromagnetic energy exists simultaneously above the grating. On the upward slope of the dispersion curve, the forward-moving energy is greater than the backward-moving energy. On the downward slope, the backward-moving energy is dominant. At the Bragg point, the forward-moving energy equals the backward-moving energy. By carefully processing the dispersion equation, we find that the growth rate does not diverge near the Bragg point, which is more reasonable than the previous theories. The Smith-Purcell free-electron is distinguished into TWT-type and BWO-type according to its operation manner in previous theories. But, in our theory, the interaction mechanism is same, therefore, the device can oscillate without external reflections on the downward slope, the Bragg point and the upward slope of the dispersion relation when the beam current beyond the start current. We develop a simple method to evaluate the start current based on the power flow of space harmonics, and also provide a way to convert spatial growth rate to temporal growth rate. The particle-in-cell simulations are carried out to examine the present theory, and the agreement between theoretical predictions and simulation data is reasonable. The theory proposed in this paper is applicable not only to Smith–Purcell free-electron lasers, but also to devices like TWTs and BWOs.

Acknowledgment

This work is partially supported by KAKENHI (No. 24560057); Research Foundation for Opto-Science and Technology; a Grant-in-Aid for Scientific Research on Innovative Areas "Electromagnetic Metamaterials" (No. 22109003) from The Ministry of Education, Culture, Sports, Science and Technology (MEXT), Japan; the National Natural Science Foundation of China (No. 61271029 and 10975031); The National High Technology Research and Development Program of China (No. 2011AA010204); and the Fundamental Research Funds for the Central Universities (No. ZYGX2009Z003).

References

[1] S.J. Smith and E.M. Purcell. *Phys. Rev.* 92, 1069 (1953).

[2] A. Gover and Z. Livni. *Opt. Commun*. 26, 375 (1978).

[3] L. Schachter and A. Ron. *Phys. Rev*. A 40, 876 (1989).

[4] R.P. Leavitt, D.E. Wortman, and C.A. Morrison. *Appl. Phys. Lett*. 35, 363 (1979).

[5] K. Mizuno, S. Ono, and Y. Shibata. *IEEE Trans. Electron*. Dev. ED-20, 749 (1973).

[6] J. Urata, M. Goldstein, M.F. Kimmitt, et. al.. *Phys. Rev. Lett*. 80, 516 (1998).

[7] H.L. Andrews, C.H. Boulware, C.A. Brau, et. al.. *Phys. Rev.* ST Accel. Beams 7, 070701 (2004).

[8] H.L. Andrews, C.H. Boulware, C.A. Brau, et. al.. *Phys. Rev*. ST Accel. Beams 8, 050703 (2005).

[9] H.L. Andrews, C.H. Boulware, C.A. Brau, et. al.. *New J. Phys*. 8, 289 (2006).

[10] J.D. Jarvis, H.L. Andrews, and C.A. Brau. *Phys. Rev*. ST Accel. Beams 13, 020701 (2010).

[11] Kwang-Je Kim and Vinit Kumar. *Phys. Rev*. ST Accel. Beams 10, 080702 (2007).

[12] Vinit Kumar and Kwang-Je Kim. *Phys. Rev*. E 73, 026501 (2006).

[13] Vinit Kumar and Kwang-Je Kim. *Phys. Rev*. ST Accel. Beams 12, 070703 (2009).

[14] H.L. Andrews, C.H. Boulware, C.A. Brau, et. al.. *Phys. Rev.* ST Accel. Beams 8, 110702 (2005).

[15] R. Kompfner and N.T. Williams. *Proc. IRE* 41, 1602(1953).

[16] J.A. Swegle. *Phys. Fluids* 30, 1201 (1987).

[17] N.S. Gizburg, S.P. Kuznetzov, and T.N. Fedoseeva. *Sov. Radiophys* 21, 728 (1979).

[18] J. Gardelle, P. Modin, and J.T. Donohue. *Phys. Rev. Lett*. 105, 224801 (2010).

[19] D. Li, Z. Yang, Y. Tsunawaki, et. al.. *Appl. Phys. Lett.* 98, 221503 (2011).

[20] D. Li, M. Hangyo,Y. Tsunawaki, et. al.. *Appl. Phys. Lett.* 100, 191101 (2012).

[21] G.F. Mkrtchian. *Phys. Rev*. ST Accel. Beams 10, 080701 (2007).

[22] T. Shiozawa, *Classical Relativistic Electrodynamics* (Springer, 2004).

[23] J.T. Donohue and J. Gardelle. *Phys. Rev.* ST Accel. Beams 9, 060701 (2006).

[24] D. Li, Z. Yang, K. Imasaki, et. al.. Phys. Rev. ST Accel. Beams 9, 040701 (2006).

[25] J.T. Donohue and J. Gardelle. *Phys. Rev*. ST Accel. Beams 8, 060702 (2005).

[26] D. Li, K. Imasaki, X. Gao, et. al.. *Appl. Phys. Lett*. 91, 221506 (2007).

[27] D. Li, K. Imasaki, Z. Yang, et. al.. *Appl. Phys. Lett*. 88, 201501 (2006).

[28] Di Jun, Zhu Da-jun, Liu Sheng-gang. *Electromagnetic Field Algorithm of the CHIPIC Code* (2005)